CPC(HEP & NP), 2009, **33**(X): 1—11 **Chinese Physics C** Vol. 33, No. X, Xxx, 2009

arXiv:1105.1620v2 [hep-ph] 8 Jul 2011

Study on the mechanism of open-flavor strong decays

LI Bao-Fei[1] CHEN Xiao-Lin[2] DENG Wei-Zhen[1;1)]

1 (Department of Physics and State Key Laboratory of Nuclear Physics and Technology,
Peking University, Beijing 100871, China)
2 (Department of Physics, Peking University, Beijing 100871, China)

Abstract The open-flavor strong decays are studied based on the interaction of potential quark model. The decay process is related to the s-channel contribution of the same scalar confinement and one-gluon-exchange(OGE) interaction in the quark model. After we adopt the prescription of massive gluons in time-like region from the lattice calculation, the approximation of four-fermion interaction is applied. The numerical calculation is performed to the meson decays in u, d, s light flavor sector. The analysis of the D/S ratios of $b_1 \to \omega\pi$ and $a_1 \to \rho\pi$ shows that the scalar interaction should be dominant in the open-flavor decays.

Key words hadron decay, four-fermion interaction, quark potential model

PACS 13.25.-k, 12.39.Pn

1 Introduction

Although QCD is considered a correct theory for strong interactions, knowledge about the hadron structure in low energy region is restricted due to the color confinement. The potential quark model is widely used to identify the conventional hadron states in hadron physics. In contrary to its impressive success in hadron spectra, especially when heavy quarks are involved, its interpretation to the hadron strong decays is unsatisfied. Although there exist some phenomenological models for the strong decays, the relationship between these models and the potential quark model is somewhat obscure.

One of the most popular models for open-flavor strong decays is $^3P_0$ model developed in the 1970s [1, 2]. This model has successfully demonstrated its universal practical utility when applied to a great number of particular decay channels [3–7]. Later the flux-tube-breaking model was proposed and $^3P_0$ model could be regarded as a limiting case of this improved model [8]. As early as 1978, Eichten et al. [9] developed the Cornell model by incorporating the possibility of creation of a light-quark pair into the quark model Hamiltonian. However, in their model they considered the quark interaction the time-component part of the vector interaction and assumed that the interaction of the quark pair creation was the same as the instantaneous interaction between two constituent quarks. In recent years an extended model including the scalar confining and vector OGE interactions was studied by E.S.Ackleh et al. [10]. A similiar scalar color-singlet confining interaction was dervied from a relativistic string breaking kernel [11].

The instantaneous interaction in the above models always assumes Breit approximation when dealing with gluon's momentum. For the potentials in quark model, the energy of the exchanged gluon is negligible as compared with the the masses of constituent quarks. Therefore the transferred gluon momentum is space-like. Nevertheless, it is in all the probability time-like if considering the creation of quark-antiquark pair by the gluons. Besides, based on the recent study in lattice field theory [12, 13], gluons are supposed to act as massive vector bosons in non-perturbative region with masses evaluated about 600∼1000MeV. A non-vanishing gluon mass is also needed in the phenomenological calculation of the diffractive scattering [14] and radiative decays of the J/ψ and Υ [15].

In this paper, an alternative study of the open-flavor strong decays is taken and inspected by the experimental decay widths. Following Ref. [10], the quark pair-creation interaction consists of a scalar confining interaction and an OGE part. We will distinguish the Breit approximation of the gluon's propagator in the time-like region from that in the space-like region. In the time-like non-perturbative region,

---

Received January 20, 2013

1) E-mail: dwz@pku.edu.cn

©2009 Chinese Physical Society and the Institute of High Energy Physics of the Chinese Academy of Sciences and the Institute

the massive gluon prescription is adopted according to Refs. [12, 13]. In this way, the decay interaction will be further simplified to the form of four-fermion interaction.

2 The Decay Model

To describe the creation of a light-quark pair in the quark model, a plausible approach is to consider the field quantization of the quark potential. In the Cornell model, the quark potential is replaced by an instantaneous interaction [9]

$$H_I = \frac{1}{2}\int d^3x d^3y : \rho_a(\boldsymbol{x})\frac{3}{4}V(\boldsymbol{x}-\boldsymbol{y})\rho_a(\boldsymbol{y}) : . \qquad (1)$$

where

$$\rho_a(\boldsymbol{x}) = \sum_{\text{flavors}} \psi^\dagger(\boldsymbol{x}) T_a \psi(\boldsymbol{x}). \qquad (2)$$

is the quark color-charge-density operator. Here $\psi(x)$ denotes the quark field with flavor and color indices suppressed, and T_a stands for the Gell-Mann matrices for $SU(3)$ generators. Since the confinement should be the Lorentz scalar, in Ref. [10] the instantaneous interaction is replaced by the combination of the scalar confinement interaction and the vector OGE interaction.

We will start from the covariant nonlocal current-current action of the quark interaction [16]:

$$A = -\frac{1}{2}\int d^4x d^4y \bar{\psi}(x)\gamma_\mu T_a \psi(x) G(x-y) \bar{\psi}(y)\gamma^\mu T_a \psi(y) - \frac{1}{2}\int d^4x d^4y \bar{\psi}(x) T_a \psi(x) S(x-y) \bar{\psi}(y) T_a \psi(y). \qquad (3)$$

The vector kernel $G(x-y)$ corresponds to the gluon propagator in coordinate space which generates the OGE Coulomb potential $-\frac{\alpha_s}{r}$ in the quark model. In the momentum space

$$G(q^2) = -\frac{4\pi\alpha_s}{q^2}. \qquad (4)$$

On the other hand, the scalar kernel $S(x-y)$ should generate the linear confining potential $\frac{3}{4}br$. Thus in the momentum space

$$S(q^2) = -\frac{6\pi b}{q^4}. \qquad (5)$$

The relevant coupling constants α_s and b are the potential parameters in the potential quark model.

The lattice calculation shows that the behavior of the gluon propagator is quite different in the non-perturbative region. In Refs. [12, 13], the transverse propagator is assumed to be:

$$D(q^2) = \frac{Z(q^2)}{q^2 - M^2(q^2)}. \qquad (6)$$

where $M(q^2)$ is the running gluon mass. Then the kernels G and S are modified to

$$G(q^2) = -\frac{4\pi\alpha_s}{q^2 - M^2(q^2)}. \qquad (7)$$

$$S(q^2) = -\frac{6\pi b}{[q^2 - M^2(q^2)]^2}. \qquad (8)$$

The lattice simulations suggest $M(0) = 600 \sim 1000$ MeV which means that gluon gets a non-vanishing mass M_g in the non-perturbative region $q \ll \Lambda_{\text{QCD}}$. If the q^2 term in the gluon's propagator is neglected in the quark-antiquark pair-creation process, then the decay interaction is simplified to the four-fermion interaction. The interaction Hamiltonian density for pair-creation turns to be:

where $\mathcal{H}_s(x)$ and $\mathcal{H}_v(x)$ represent the scalar and vector interaction respectively:

$$\mathcal{H}_s(x) = \frac{3\pi b}{M_g^4}\bar{\psi}(x)T_a\psi(x)\bar{\psi}(x)T^a\psi(x). \qquad (10)$$

$$\mathcal{H}_v(x) = -\frac{2\pi\alpha_s}{M_g^2}\bar{\psi}(x)\gamma_\mu T_a\psi(x)\bar{\psi}(x)\gamma^\mu T^a\psi(x). \qquad (11)$$

From the interaction in Eqs. (10) and (11), we can derive the formulae for decay rates within non-relativistic limit. As meson states are normalized to $2E$ in our work,

$$\langle \boldsymbol{p}|\boldsymbol{p}'\rangle = 2E\delta^3(\boldsymbol{p}-\boldsymbol{p}'). \qquad (12)$$

the differential decay width in two-body decay process $A \to B + C$ is expressed in terms of transition amplitude as:

$$d\Gamma = \frac{\mathcal{S}|\mathcal{M}|^2}{2E_A}(2\pi)^7\delta^4(P_A - P_B - P_C)\frac{d^3\boldsymbol{P}_B}{2E_B}\frac{d^3\boldsymbol{P}_C}{2E_C}. \qquad (13)$$

where $\mathcal{S}$ is the symmetric factor

$$\mathcal{S} = \frac{1}{1+\delta(B,C)}. \qquad (14)$$

The amplitude $\mathcal{M}$ is related to the decay interaction through:

$$\mathcal{M} = < BC|\mathcal{H}_I(0)|A> = \mathcal{M}_v + \mathcal{M}_s. \qquad (15)$$

where $\mathcal{M}_v$ and $\mathcal{M}_s$ are the amplitudes from vector and scalar interaction respectively.

For each interaction, the transition amplitude comes from four diagrams. For the vector interaction, its Feynman diagrams are shown in Figure 1.

Fig. 1. Contributions to vector interaction.

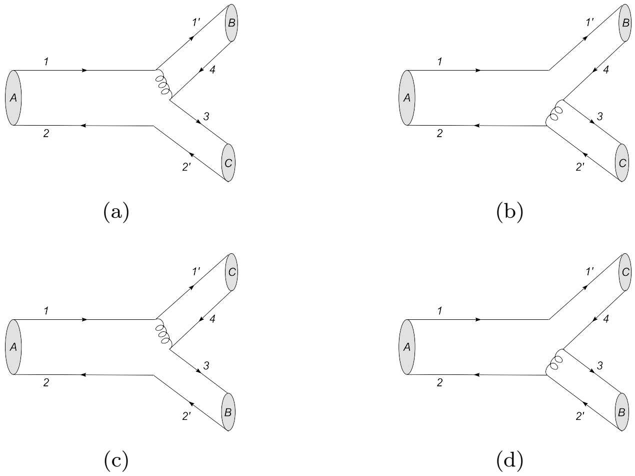

(a) (b)

(c) (d)

In Diagram (a) the $q\bar{q}$ pair is created from gluons emitted by the initial quark while in Diagram (b) the $q\bar{q}$ pair is created from gluons emitted by the initial anti-quark. Diagrams (c) and (d) come from the interchange of final particles B and C in Diagrams (a) and (b) respectively.

The total decay width is expressed as

$$\Gamma = \frac{16\pi^7 \mathcal{S} P_f}{M_A^2} \sum_{LS} |\mathcal{M}^{LS}|^2. \tag{16}$$

where $\boldsymbol{P}_f = \boldsymbol{P}_B = -\boldsymbol{P}_C$ in the rest frame of initial particle A and $\mathcal{M}^{LS}$ are the partial wave amplitudes.

For further simplification, the space wave functions of all meson states are taken to be the simple harmonic oscillator (SHO) wave functions with a common oscillator parameter β. The partial wave amplitudes $\mathcal{M}^{LS}$ are presented in the appendix.

3 Results and Analysis

In the numerical calculation, the common oscillator parameter $\beta = 400$MeV is adopted from Ref. [16]. All related masses of mesons are taken from Ref. [17]. Other parameters, like constituent quark masses, coupling constants α_s and b are also taken from Ref. [16]. They are $m_u = m_d = 220$MeV, $m_s = 419$MeV, $\alpha_s = 0.60$, and $b = 0.18\text{GeV}^2$ respectively.

The only one parameter which cannot be determined from the quark model is the effective gluon mass M_g. In this work, this parameter is fixed in a least square fit to the experimental decay widths. We find that $M_g = 668$MeV which falls within the range $600 \sim 1000$MeV estimated in the lattice calculation [12, 13].

The results of the decay widths are tabulated in Table 1 together with the decay widths of $^3P_0$ model and the experimental data. In the table, Γ_1 indicates the decay rates of our calculation. As can been seen, the widths of the decay processes characterized by the creation of $s\bar{s}$ pair are rather small compared with the experimental data. The reason is that the creation of $s\bar{s}$ pair is suppressed in the four-fermion interaction due to the heavier mass of s quark. Note that in the $^3P_0$ model, the transition operator is independent of the flavor mass in $q\bar{q}$ pair creation. This shows that the $q\bar{q}$ pair creation has the flavor $SU(3)$ symmetry. In the third column Γ_2 in Table 1, the decay widths related to $s\bar{s}$ pair creation are recalculated with the flavor symmetry restored with $m_s = m_u = 220$MeV in the decay Hamiltonian. The corresponding decay widths are enhanced which improves the fit to the experimental data.

Table 1. The decay widths. The decay widths of $^3P_0$ model are taken from Ref. [3]. The experimental data are taken from Ref. [17]. Unit: MeV

Channel	Γ_1	Γ_2	Γ_3	$^3P_0$	Exp
$\rho \to \pi\pi$	109.7		138	96	149
$b_1 \to \omega\pi$	57.7		160	176	142
$a_2 \to \rho\pi$	51.5		49.7	65	75.4
$a_2 \to \eta\pi$	15.4		19.5		15.5
$a_2 \to K\bar{K}$	1.64	9.03	2.26	11	5.24
$a_2 \to \eta'\pi$	1.20		1.52		0.567
$\pi_2 \to f_2\pi$	58.6		77.1	147	146
$\pi_2 \to \rho\pi$	58.3		128	232	80.3
$\pi_2 \to K^*\bar{K}+c.c.$	0.23	10.8	4.66	38	10.9
$\pi_2 \to \rho\omega$	9.23		25.1		7.00
$\rho_3 \to \pi\pi$	47.3		59.6	116	38.0
$\rho_3 \to \omega\pi$	17.8		17.2	36	25.8
$\rho_3 \to K\bar{K}$	0.68	7.06	0.94	9.2	2.54
$f_2 \to \pi\pi$	136		172	203	157
$f_2 \to K\bar{K}$	1.07	5.98	1.48	7.2	8.51
$f_4 \to \omega\omega$	23.9		14.9	53	54
$f_4 \to \pi\pi$	27.6		34.8	123	40.3
$f_4 \to K\bar{K}$	0.18	3.45	0.25	5.4	1.61
$f_0(1500) \to \pi\pi$	108		34.7		38.0
$f_0(1500) \to K\bar{K}$	4.95	7.99	0.49		9.38
$\phi \to K^+K^-$	1.96	2.63	2.18	2.37	2.10
$f_2' \to K\bar{K}$	84.3	78.9	21.0	117	64.8
$K^* \to K\pi$	41.7	45.9	46.4	36	50.8
$K^*(1410) \to K\pi$	21.7	32.4	1.15		15.3
$K_0^* \to K\pi$	348	1062	194	163	251
$K_2^* \to K\pi$	81.7	73	90.2	108	49.2
$K_2^* \to K^*\pi$	23.0	20.3	20.6	27	24.3
$K_2^* \to K\rho$	7.22	6.20	6.42	9.3	8.57
$K_2^* \to K\omega$	2.12	1.82	1.88	2.6	2.86
$K_3^* \to K\rho$	14.4	9.54	12.5	24	49.3
$K_3^* \to K^*\pi$	19.5	13.8	17.7	33	31.8
$K_3^* \to K\pi$	45.1	32	49.4	87	30.0
$K_4^* \to K\pi$	18.4	10.1	20	55	19.6
$K_4^* \to K^*\phi$	0.37	2.44	0.23	3.2	2.8

Individual decay amplitudes from scalar and vector interactions are listed in Table 2. The scalar interaction is dominant in most of the decay channels. However in the channels $1D \to 1P+1S$, $2S \to 1S+1S$ and $2P \to 1S+1S$ the contribution from the vector interaction is important, while in the channel $^3P_0 \to {}^1S_0+{}^1S_0$ the vector interaction becomes dominant, as can be seen in the process $f_0(1370) \to \pi\pi$ whose decay width may amount to 1000 MeV which is too large compared with the experimental result of $200-500$MeV.

Table 2. The individual amplitudes from scalar and vector interactions. Unit: MeV

channel	L	S	M_s	M_v	M
$\rho\to\pi\pi$	P	0	-1.39	-0.55	-1.94
$b_1\to\omega\pi$	S	1	2.34	-0.35	2.00
$b_1\to\omega\pi$	D	1	0.62	0.49	1.11
$a_2\to\rho\pi$	D	1	-1.32	-0.79	-2.11
$a_2\to\eta\pi$	D	0	-0.73	-0.29	-1.02
$a_2\to K\bar{K}$	D	0	-0.28	-0.09	-0.36
$a_2\to\eta'\pi$	D	0	-0.28	-0.11	-0.39
$\pi_2\to f_2\pi$	S	2	2.32	-5.52	-3.20
$\pi_2\to f_2\pi$	D	2	0.383	-0.003	0.380
$\pi_2\to f_2\pi$	G	2	0.01	0.004	0.014
$\pi_2\to\rho\pi$	P	1	1.85	-0.72	1.14
$\pi_2\to\rho\pi$	F	1	1.10	0.88	1.98
$\pi_2\to K^*\bar{K}+c.c.$	P	1	0.49	-0.56	-0.07
$\pi_2\to K^*\bar{K}+c.c.$	F	1	0.09	0.07	0.16
$\pi_2\to\rho\omega$	P	1	1.39	-0.09	1.31
$\pi_2\to\rho\omega$	F	1	0.13	0.10	0.23
$\rho_3\to\pi\pi$	F	0	-1.31	-0.52	-1.83
$\rho_3\to\omega\pi$	F	1	-0.80	-0.47	-1.27
$\rho_3\to K\bar{K}$	F	0	-0.18	-0.06	-0.24
$f_2\to\pi\pi$	D	0	-1.95	-0.77	-2.72
$f_2\to K\bar{K}$	D	0	-0.23	-0.08	-0.31
$f_4\to\omega\omega$	G	0	-0.08	-0.03	-0.11
$f_4\to\omega\omega$	D	2	0.88	0.87	1.75
$f_4\to\omega\omega$	G	2	0.15	0.15	1.30
$f_4\to\pi\pi$	G	0	-1.09	-0.43	-1.52
$f_4\to K\bar{K}$	G	0	-0.10	-0.03	-0.13
$f_0(1500)\to\pi\pi$	S	0	0.95	-3.56	-2.61
$f_0(1500)\to K\bar{K}$	S	0	0.13	-0.77	-0.64
$\phi\to K^+K^-$	P	0	-0.40	-0.20	-0.60
$f_2'\to K\bar{K}$	D	0	-0.84	-0.28	-1.12
$K^*\to K\pi$	P	0	-1.04	-0.50	-1.54
$K^*(1410)\to K\pi$	P	0	-0.18	1.39	1.21
$K_0^*\to K\pi$	S	0	-2.32	7.19	4.87
$K_2^*\to K\pi$	D	0	-1.58	-0.78	-2.36
$K_2^*\to K^*\pi$	D	1	0.92	0.61	1.52
$K_2^*\to K\rho$	D	1	-0.59	-0.39	-0.98
$K_2^*\to K\omega$	D	1	-0.32	-0.21	-0.53
$K_3^*\to K\rho$	F	1	-0.74	-0.50	-1.24
$K_3^*\to K^*\pi$	F	1	0.74	0.44	1.18
$K_3^*\to K\pi$	F	0	-1.27	-0.63	-1.90
$K_4^*\to K\pi$	G	0	-0.86	-0.43	-1.29
$K_4^*\to K^*\phi$	G	0	-0.003	-0.002	-0.005
$K_4^*\to K^*\phi$	D	2	0.15	0.15	0.30
$K_4^*\to K^*\phi$	G	2	0.007	0.007	0.014

One of the important criteria for the strong decay models is the D/S amplitude ratios in the decays $b_1\to\omega\pi$ and $a_1\to\rho\pi$. Experimentally, these ratios are $D_1=0.277\pm0.027$ and $D_2=-0.062\pm0.02$ respectively [17]. In the current model, analytic expressions for these ratios are:

$$D_1 \;=\; -\frac{\sqrt{2}p_f^2(15b+8m_g^2\alpha)}{15bp_f^2+8m_g^2p_f^2\alpha-72b\beta^2}. \tag{17}$$

$$D_2 \;=\; \frac{\sqrt{2}p_f^2(5b+2\alpha m_g^2)}{2b(5p_f^2-24\beta^2)+4\alpha m_g^2(p_f^2+8\beta^2)}. \tag{18}$$

According to the preceding values of the model parameters, the ratios' numerical results are: $D_1=0.566$ and $D_2=0.731$. It is apparent that D_1 is about two times larger than the experimental value while the calculated value of D_2 has a wrong sign. Since the β value is dependent on the wave function of meson, in Figure 2 we show the dependence of the ratios on β.

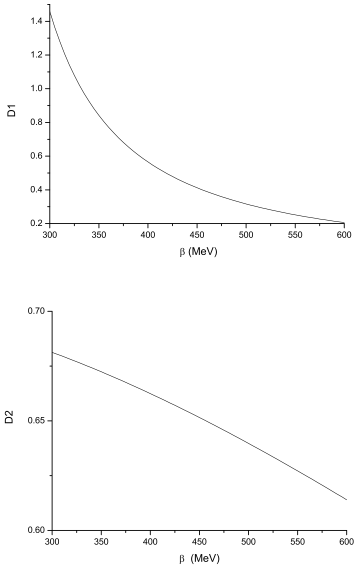

Fig. 2. D/S ratios for D_1 and D_2.

With respect to D_1 ratio, it decreases with an increasing β. When β rises up to 524MeV, the ratio regenerates the experimental value 0.277. Nonetheless, as to D_2 ratio, the numerical value keeps its opposite sign since this ratio changes rather slowly with β.

Based on the fact of the dominance of the scalar interaction, a scalar-kernel-scalar (sKs) decay model was proposed [10]. As a result we consider only the contribution from scalar interaction while leaving the vector interaction aside. The best-fitted value for M_g now becomes 597MeV and the fitted decay widths are listed in the Γ_3 column in Table 1.

One of the advantages of considering scalar interaction alone is that the D/S ratios are greatly improved. Now these ratios turn to be:

$$D_1 = -\frac{5\sqrt{2}p_f^2}{5p_f^2 - 24\beta^2}. \tag{19}$$

$$D_2 = \frac{5p_f^2}{\sqrt{2}(5p_f^2 - 24\beta^2)}. \tag{20}$$

We obtain $D_1 = 0.264$ and $D_2 = -0.140$ when $\beta = 400$MeV, well fit to the experimental results. Another improvement lies in the specific channel, ${}^3P_0 \to {}^1S_0 + {}^1S_0$. As in the process $f_0(1370) \to \pi\pi$, with the negligence of vector interaction, the decay width becomes a reasonable value 318.5MeV.

4 Summary

To summarize, we have studied a decay model based on the potential quark model. The model incorporates the decay interactions of scalar and vector quark currents which are in accordance with the confining and OGE potentials in the quark model. In the non-relativistic limit, the massive gluon propagator is assumed and the decay interactions are reduced to four fermion interactions. In this framework, we have calculated 34 decay channels. The results fit the experimental data comparable to the popular ${}^3P_0$ decay model if the $SU(3)$ flavor symmetry is assumed in the decay processes. Meanwhile the results also show the dominance of the scalar interaction in most of the decay channels. Besides, the scalar interaction is also preferred by the D/S ratios of $b_1 \to \omega + \pi$ and $a_1 \to \rho + \pi$. Thus we have calculated decay widths with only scalar interaction (the sKs model which is quite similar to the ${}^3P_0$ model since the $q\bar{q}$ scalar current produces a ${}^3P_0$ quark pair). It seems that scalar interaction alone is able to give a crude estimation of most decay widths.

We would like to thank Prof. Shi-Lin Zhu for useful discussions.

Appendix

A Amplitudes and Overlapping Integrals for Some Channels

The partial wave decay amplitude $A \to B + C$ can be expressed as

$$\mathcal{M}^{LS} = \frac{\sqrt{8E_AE_BE_C}}{24\pi^5} C_f M^{LS}. \tag{A1}$$

where C_f is the flavor factor:

$$C_f^2 = (2T_B+1)(2T_C+1) \begin{Bmatrix} T_A & T_B & T_C \\ t & t_2 & t_1 \end{Bmatrix}^2. \tag{A2}$$

where T_A, T_B, T_C are the iso-spins of mesons A, B, C, respectively. t_1, t_2, t are the iso-spins of quarks labeled as 1, 2, 3 in Figure 1, respectively. Similarly, in the following, the masses of quarks 1, 2, 3 will be denoted by m_1, m_2, m, respectively.

The decay amplitudes M^{LS} can be split into two parts which include scalar M_s^{LS} and vector M_v^{LS}. Furthermore, each M_i^{LS} would part into four components:

$$M_i^{LS} = M_i^{LS}(a) + M_i^{LS}(b) + M_i^{LS}(c) + M_i^{LS}(d). \qquad \text{(A3)}$$

according to Figure 1. In the following, we will only present the formulae for $M_i^{LS}(a)$. $M_i^{LS}(b)$ is related to $M_i^{LS}(a)$ by a charge conjugate:

$$\begin{aligned} M_i^{LS}(b; A \to B + C) &= (-1)^{J_B + J_C - S + S_A + S_B + S_C + 1} \\ &\quad \times M_i^{LS}(a; \bar{A} \to \bar{C} + \bar{B}). \qquad \text{(A4)} \end{aligned}$$

where $\bar{A}$, $\bar{B}$, $\bar{C}$ are the charge conjugates of A, B, C, respectively. The $M_i^{LS}(c)$, $M_i^{LS}(d)$ are related to $M_i^{LS}(a)$, $M_i^{LS}(b)$ by the exchange of final particles B and C.

Since the decay interaction is four-fermion interaction, the spatial overlap integrals involve:

$$\begin{aligned} p_{AC}(m_A, m_C) &= \int d\boldsymbol{k} \psi^*_{n_C l_C m_C}(\boldsymbol{k}) \\ &\quad \times \psi_{n_A l_A m_A}(\boldsymbol{k} + \xi p_f \hat{\boldsymbol{z}}). \\ v_{AC}(m_A, m_C, m) &= \int d\boldsymbol{k} \psi^*_{n_C l_C m_C}(\boldsymbol{k}) \\ &\quad \times \psi_{n_A l_A m_A}(\boldsymbol{k} + \xi p_f \hat{\boldsymbol{z}}) k_m. \\ p_B(m_B) &= \int d\boldsymbol{k} \psi^*_{n_B l_B m_B}(\boldsymbol{k}). \\ v_B(m_B, m) &= \int d\boldsymbol{k} \psi^*_{n_B l_B m_B}(\boldsymbol{k}) k_m. \qquad \text{(A5)} \end{aligned}$$

where $\xi = \frac{m_2}{m_2 + m}$, and

$$k_m = \begin{cases} -\frac{1}{\sqrt{2}}(k_x + i k_y) & m = 1 \\ k_z & m = 0 \\ +\frac{1}{\sqrt{2}}(k_x - i k_y) & m = -1 \end{cases} \qquad \text{(A6)}$$

All the spatial wave functions ψ_{nlm} are taken to be the simple harmonic oscillator (SHO) wave functions with the oscillator parameters β_A, β_B, β_C for mesons A, B, C respectively. We have

$$p_B(m_B) = \frac{\delta(l_B, 0)}{n_B!} (4\pi \beta_B^2)^{\frac{3}{4}}. \qquad \text{(A7)}$$

$$v_B(m_B, m) = \frac{\delta(l_B, 1)\delta(m_B, m)}{n_B!} 4\pi^{\frac{3}{4}} \beta_B^{\frac{5}{2}}. \qquad \text{(A8)}$$

Let

$$\eta \equiv \left(\frac{2\beta_A \beta_C}{\beta_A^2 + \beta_C^2} \right)^{\frac{3}{2}} e^{-\frac{\xi^2 p_f^2}{2(\beta_A^2 + \beta_C^2)}}. \qquad \text{(A9)}$$

Below we list the non-vanishing integrals p_{AC} and v_{AC} relevant to our work.

- $1S \to 1S$

$$\begin{aligned} p_{AC}(0,0) &= \eta \\ v_{AC}(0,0,0) &= -\frac{\xi \eta \beta_C^2}{\beta_A^2 + \beta_C^2} p_f \end{aligned}$$

- $2S \to 1S$

$$\begin{aligned} p_{AC}(0,0) &= \frac{(3\beta_A^4 - 3\beta_C^4 - 2p_f^2 \beta_A^2 \xi^2)\eta}{\sqrt{6}(\beta_A^2 + \beta_C^2)^2} \\ v_{AC}(0,0,0) &= \frac{p_f \beta_C^2 \xi \eta}{\sqrt{6}(\beta_A^2 + \beta_C^2)^3}(-7\beta_A^4 + 3\beta_C^4 \\ &\quad -4\beta_A^2 \beta_C^2 + 2p_f^2 \xi^2 \beta_A^2) \end{aligned}$$

- $1P \to 1S$

$$\begin{aligned} p_{AC}(0,0) &= \frac{\sqrt{2}\eta \xi \beta_A p_f}{\beta_A^2 + \beta_C^2} \\ v_{AC}(0,0,0) &= \frac{\sqrt{2}\eta \beta_A \beta_C^2 (\beta_A^2 + \beta_C^2 - p_f^2 \xi^2)}{(\beta_A^2 + \beta_C^2)^2} \\ v_{AC}(1,0,-1) &= v_{AC}(-1,0,1) = \frac{-\sqrt{2}\eta \beta_A \beta_C^2}{(\beta_A^2 + \beta_C^2)} \end{aligned}$$

- $1D \to 1S$

$$\begin{aligned} p_{AC}(0,0) &= \frac{2p_f^2 \beta_A^2 \xi^2 \eta}{\sqrt{3}(\beta_A^2 + \beta_C^2)^2} \\ v_{AC}(0,0,0) &= \frac{2p_f \beta_A^2 \beta_C^2 \xi \eta (2\beta_A^2 + 2\beta_C^2 - p_f^2 \xi^2)}{\sqrt{3}(\beta_A^2 + \beta_C^2)^3} \\ v_{AC}(1,0,-1) &= v_{AC}(-1,0,1) = \frac{-2p_f \beta_A^2 \beta_C^2 \eta \xi}{(\beta_A^2 + \beta_C^2)^2} \end{aligned}$$

- $1D \to 1P$

$$\begin{aligned} p_{AC}(0,0) &= \frac{2\sqrt{2}p_f \xi \eta \beta_A^2 \beta_C (2\beta_A^2 + 2\beta_C^2 - p_f^2 \xi^2)}{\sqrt{3}(\beta_A^2 + \beta_C^2)^3} \\ p_{AC}(1,1) &= p_{AC}(-1,-1) = \frac{2\sqrt{2}p_f \eta \xi \beta_A^2 \beta_C}{(\beta_A^2 + \beta_C^2)^2} \\ v_{AC}(0,0,0) &= \frac{2\sqrt{2}\beta_A^2 \beta_C \eta}{\sqrt{3}(\beta_A^2 + \beta_C^2)^4}[2\beta_C^6 - 4p_f^2 \beta_C^4 \xi^2 + p_f^4 \beta_C^2 \xi^4 + \beta_A^4(2\beta_C^2 + p_f^2 \xi^2) + \beta_A^2(4\beta_C^4 - 3p_f^2 \beta_C^2 \xi^2)] \\ v_{AC}(2,1,-1) &= v_{AC}(-2,-1,1) = -\frac{4\beta_A^2 \beta_C^3 \eta}{(\beta_A^2 + \beta_C^2)^2} \\ v_{AC}(1,0,-1) &= v_{AC}(-1,0,1) = -\frac{2\sqrt{2}\beta_A^2 \beta_C^3 \eta (\beta_A^2 + \beta_C^2 - \xi^2 p_f^2)}{(\beta_A^2 + \beta_C^2)^3} \\ v_{AC}(1,1,0) &= v_{AC}(-1,-1,0) = -v_{AC}(1,0,-1) \end{aligned}$$

$$v_{AC}(0,1,1) = v_{AC}(0,-1,-1) = -\frac{2\sqrt{2}\eta\beta_A^2\beta_C[\beta_C^4+\beta_A^2(\beta_C^2-\xi^2p_f^2)]}{\sqrt{3}(\beta_A^2+\beta_C^2)^3}$$

- $1F \to 1S$

$$\begin{aligned}
p_{AC}(0,0) &= \frac{2\sqrt{2}\eta\xi^3\beta_A^3p_f^3}{\sqrt{15}(\beta_A^2+\beta_C^2)^3}\\
v_{AC}(0,0,0) &= \frac{2\sqrt{2}\eta p_f^2\beta_A^3\beta_C^2\xi^2(3\beta_A^2+3\beta_C^2-p_f^2\xi^2)}{\sqrt{15}(\beta_A^2+\beta_C^2)^4}\\
v_{AC}(1,0,-1) &= v_{AC}(-1,0,1) = \frac{-4\eta p_f^2\beta_A^3\beta_C^2\xi^2}{\sqrt{5}(\beta_A^2+\beta_C^2)^3}
\end{aligned}$$

We further introduce some useful combinations:

$$A_L = p_f p_B(0)\sum_{m_A m_C} p_{AC}(m_A,m_C)\,\langle l_C m_C L0|l_A m_A\rangle \tag{A10}$$

$$B_{LJ} = \sqrt{2l_A+1}p_B(0)\sum_{m_A m_C m} v_{AC}(m_A,m_C,m)\,\langle l_C m_C L0|Jm_C\rangle\,\langle l_A m_A 1m|Jm_C\rangle \tag{A11}$$

The relevant partial wave amplitudes are given in subsections.

A.1 $S \to S+S$

- ${}^3S_1 \to {}^1S_0 + {}^1S_0$

$$\begin{aligned}
M_s^{10}(a) &= -\frac{\sqrt{\pi}b}{\sqrt{2}M_g^4}\left[(\frac{1}{m+m_1}+\frac{1}{m+m_2})A_0-\frac{1}{m}B_{11}\right]\\
M_v^{10}(a) &= -\frac{\sqrt{2\pi}\alpha_s}{3M_g^2}\left[\frac{m_1(m_1+m_2)-m(m_1-3m_2)}{m_1(m+m_1)(m+m_2)}A_0+(\frac{3}{m_1}-\frac{1}{m})B_{11}\right]
\end{aligned}$$

- ${}^3S_1 \to {}^3S_1 + {}^1S_0$

$$\begin{aligned}
M_s^{11}(a) &= \sqrt{2}M_s^{10}(a;{}^3S_1\to{}^1S_0+{}^1S_0)\\
M_v^{11}(a) &= -\frac{2\sqrt{\pi}\alpha_s}{3M_g^2}\left[(\frac{m_1+m_2}{m_1(m+m_2)})A_0+(\frac{1}{m_1}-\frac{1}{m})B_{11}\right]
\end{aligned}$$

- ${}^3S_1 \to {}^1S_0 + {}^3S_1$

$$\begin{aligned}
M_s^{11}(a) &= -\sqrt{2}M_s^{10}(a;{}^3S_1\to{}^1S_0+{}^1S_0)\\
M_v^{11}(a) &= -\sqrt{2}M_v^{10}(a;{}^3S_1\to{}^1S_0+{}^1S_0)
\end{aligned}$$

- ${}^1S_0 \to {}^3S_1 + {}^1S_0$

$$\begin{aligned}
M_s^{11}(a) &= -\sqrt{3}M_s^{10}(a;{}^3S_1\to{}^1S_0+{}^1S_0)\\
M_v^{11}(a) &= \frac{\sqrt{2\pi}\alpha_s}{\sqrt{3}M_g^2}\left[\frac{m(3m_1-m_2)+m_1(m_1+m_2)}{m_1(m+m_1)(m+m_2)}A_0-(\frac{1}{m}+\frac{1}{m_1})B_{11}\right]
\end{aligned}$$

- ${}^1S_0 \to {}^1S_0 + {}^3S_1$

$$\begin{aligned}
M_s^{11}(a) &= -\sqrt{3}M_s^{10}(a;{}^3S_1\to{}^1S_0+{}^1S_0)\\
M_v^{11}(a) &= -\sqrt{3}M_v^{10}(a;{}^3S_1\to{}^1S_0+{}^1S_0)
\end{aligned}$$

A.2 $P\rightarrow S+S$

- ${}^3P_0\rightarrow{}^1S_0+{}^1S_0$

$$\begin{aligned}
M_s^{00}(a) &= \frac{\sqrt{\pi}b}{\sqrt{2}M_g^4}\left[(\frac{1}{m+m_1}+\frac{1}{m+m_2})A_1+\frac{1}{m}B_{00}\right]\\
M_v^{00}(a) &= \frac{\sqrt{2\pi}\alpha_s}{3M_g^2}\left[\frac{m_1(m_1-m)+m_2(m_1+3m)}{m_1(m+m_1)(m+m_2)}A_1-(\frac{3}{m_1}-\frac{1}{m})B_{00}\right]
\end{aligned}$$

- ${}^3P_2\rightarrow{}^1S_0+{}^1S_0$

$$\begin{aligned}
M_s^{20}(a) &= -\frac{\sqrt{\pi}b}{\sqrt{5}M_g^4}\left[(\frac{1}{m+m_1}+\frac{1}{m+m_2})A_1-\frac{\sqrt{2}}{2m}B_{22}\right]\\
M_v^{20}(a) &= -\frac{\sqrt{\pi}\alpha_s}{3\sqrt{5}M_g^2}\left[\frac{2m_1(m_1-m)+2m_2(m_1+3m)}{m_1(m+m_1)(m+m_2)}A_1+\sqrt{2}(\frac{3}{m_1}-\frac{1}{m})B_{22}\right]
\end{aligned}$$

- ${}^3P_2\rightarrow{}^3S_1+{}^1S_0$

$$\begin{aligned}
M_s^{21}(a) &= \frac{\sqrt{6}}{2}M_s^{20}(a;{}^3P_2\rightarrow{}^1S_0+{}^1S_0)\\
M_v^{21}(a) &= -\frac{\sqrt{\pi}\alpha_s}{\sqrt{30}M_g^2}\left[\frac{2(m_1+m_2)}{m_1(m+m_2)}A_1+\sqrt{2}(\frac{1}{m_1}-\frac{1}{m})B_{22}\right]
\end{aligned}$$

- ${}^3P_2\rightarrow{}^1S_0+{}^3S_1$

$$\begin{aligned}
M_s^{21}(a) &= -\frac{\sqrt{6}}{2}M_s^{20}(a;{}^3P_2\rightarrow{}^1S_0+{}^1S_0)\\
M_v^{21}(a) &= \frac{\sqrt{\pi}\alpha_s}{\sqrt{30}M_g^2}\left[\frac{2m_1(m_1-m)+2m_2(m_1+3m)}{m_1(m+m_1)(m+m_2)}A_1+\sqrt{2}(\frac{3}{m_1}-\frac{1}{m})B_{22}\right]
\end{aligned}$$

A.3 $D\rightarrow S+S$

- ${}^1D_2\rightarrow{}^3S_1+{}^3S_1$

$$\begin{aligned}
M_s^{11}(a) &= -\frac{\sqrt{3\pi}b}{5\sqrt{2}M_g^4}\left[2(\frac{1}{m+m_1}+\frac{1}{m+m_2})A_2+\frac{\sqrt{2}}{m}B_{11}\right]\\
M_v^{11}(a) &= -\frac{\sqrt{2\pi}\alpha_s}{5\sqrt{3}M_g^2}\left[\frac{2(m_1+m_2)}{m_1(m+m_2)}A_2+\sqrt{2}(\frac{1}{m}-\frac{1}{m_1})B_{11}\right]\\
M_s^{31}(a) &= \frac{\sqrt{\pi}b}{5M_g^4}\left[3(\frac{1}{m+m_1}+\frac{1}{m+m_2})A_2-\frac{\sqrt{3}}{m}B_{33}\right]\\
M_v^{31}(a) &= \frac{2\sqrt{\pi}\alpha_s}{5M_g^2}\left[\frac{m_1+m_2}{m_1(m+m_2)}A_2+\frac{1}{\sqrt{3}}(\frac{1}{m_1}-\frac{1}{m})B_{33}\right]
\end{aligned}$$

- ${}^1D_2\rightarrow{}^3S_1+{}^1S_0$

$$\begin{aligned}
M_s^{11}(a) &= \frac{1}{\sqrt{2}}M_s^{11}(a;{}^1D_2\rightarrow{}^3S_1+{}^3S_1)\\
M_v^{11}(a) &= -\frac{\sqrt{\pi}\alpha_s}{5\sqrt{3}m_g^2}\left[\frac{2m(3m_1-m_2)+2m_1(m_1+m_2)}{m_1(m+m_1)(m+m_2)}A_2+\sqrt{2}(\frac{1}{m}+\frac{1}{m_1})B_{11}\right]\\
M_s^{31}(a) &= \frac{1}{\sqrt{2}}M_s^{31}(a;{}^1D_2\rightarrow{}^3S_1+{}^3S_1)\\
M_v^{31}(a) &= \frac{\sqrt{2\pi}\alpha_s}{5m_g^2}\left[\frac{m(3m_1-m_2)+m_1(m_1+m_2)}{m_1(m+m_1)(m+m_2)}A_2-\frac{1}{\sqrt{3}}(\frac{1}{m}+\frac{1}{m_1})B_{33}\right]
\end{aligned}$$

- ${}^1D_2 \to {}^1S_0 + {}^3S_1$

$$\begin{aligned}
M_s^{11}(a) &= \frac{1}{\sqrt{2}} M_s^{11}(a;{}^1D_2 \to {}^3S_1 + {}^3S_1) \\
M_v^{11}(a) &= \frac{\sqrt{\pi}\alpha_s}{5\sqrt{3}m_g^2}\left[\frac{2m(m_1-3m_2)-2m_1(m_1+m_2)}{m_1(m+m_1)(m+m_2)}A_2+\sqrt{2}(\frac{3}{m_1}-\frac{1}{m})B_{11}\right] \\
M_s^{31}(a) &= \frac{1}{\sqrt{2}} M_s^{31}(a;{}^1D_2 \to {}^3S_1 + {}^3S_1) \\
M_v^{31}(a) &= \frac{\sqrt{2\pi}\alpha_s}{5m_g^2}\left[\frac{m_1(m_1+m_2)-m(m_1-3m_2)}{m_1(m+m_1)(m+m_2)}A_2+\sqrt{3}(\frac{1}{m_1}-\frac{1}{3m})B_{33}\right]
\end{aligned}$$

- ${}^3D_3 \to {}^1S_0 + {}^1S_0$

$$\begin{aligned}
M_s^{30}(a) &= -\frac{5}{\sqrt{70}} M_s^{31}(a;{}^1D_2 \to {}^3S_1 + {}^3S_1) \\
M_v^{30}(a) &= \frac{\sqrt{2\pi}\alpha_s}{\sqrt{35}M_g^2}\left[\frac{m(m_1-3m_2)-m_1(m_1+m_2)}{m_1(m+m_1)(m+m_2)}A_2-\sqrt{3}(\frac{1}{m_1}-\frac{1}{3m})B_{33}\right]
\end{aligned}$$

- ${}^3D_3 \to {}^3S_1 + {}^1S_0$

$$\begin{aligned}
M_s^{31}(a) &= -\sqrt{\frac{10}{21}} M_s^{31}(a;{}^1D_2 \to {}^3S_1 + {}^3S_1) \\
M_v^{31}(a) &= -2\frac{\sqrt{2\pi}\alpha_s}{\sqrt{105}M_g^2}\left[\frac{m_1+m_2}{m_1(m+m_2)}A_2+\frac{1}{\sqrt{3}}(\frac{1}{m_1}-\frac{1}{m})B_{33}\right]
\end{aligned}$$

- ${}^3D_3 \to {}^1S_0 + {}^3S_1$

$$\begin{aligned}
M_s^{31}(a) &= \sqrt{\frac{10}{21}} M_s^{31}(a;{}^1D_2 \to {}^3S_1 + {}^3S_1) \\
M_v^{31}(a) &= 2\frac{\sqrt{2\pi}\alpha_s}{\sqrt{105}M_g^2}\left[\frac{m_1(m_1-m)+m_2(m_1+3m)}{m_1(m+m_1)(m+m_2)}A_2+\sqrt{3}(\frac{1}{m_1}-\frac{1}{3m})B_{33}\right]
\end{aligned}$$

A.4 $D \to P + S$

- ${}^1D_2 \to {}^3P_2 + {}^1S_0$

$$M_s^{LS}(a) = M_v^{LS}(a) = 0$$

- ${}^1D_2 \to {}^1S_0 + {}^3P_2$

$$\begin{aligned}
M_s^{02} &= -\frac{\sqrt{\pi}b}{5\sqrt{2}mM_g^4}\left[\sqrt{3}\frac{m(m_1+m_2+2m)}{(m+m_1)(m+m_2)}A_1+B_{01}\right] \\
M_v^{02} &= -\frac{\sqrt{2\pi}\alpha_s}{15M_g^2}\left[\frac{m_1(m_1-m)+m_2(m_1+3m)}{m_1(m+m_1)(m+m_2)}\sqrt{3}A_1+(\frac{1}{m}-\frac{3}{\sqrt{2}m_1})B_{01}\right] \\
M_s^{22} &= \frac{\sqrt{\pi}b}{2\sqrt{35}mM_g^4}\left[\frac{\sqrt{2}m(m_1+m_2+2m)}{(m+m_1)(m+m_2)}A'-B'\right] \\
M_v^{22} &= \frac{\sqrt{\pi}\alpha_s}{3\sqrt{35}M_g^2}\left[\frac{\sqrt{2}[m_1(m_1-m)+m_2(m_1+3m)]}{m_1(m+m_1)(m+m_2)}A'+(\frac{3}{m_1}-\frac{1}{m})B'\right] \\
M_s^{42} &= \frac{\sqrt{6\pi}b}{10\sqrt{7}mM_g^4}\left[\frac{2\sqrt{7}m(m_1+m_2+2m)}{(m+m_1)(m+m_2)}A_3-3B_{43}\right] \\
M_v^{42} &= \frac{\sqrt{6\pi}\alpha_s}{15\sqrt{7}M_g^2}\left[\frac{2\sqrt{7}[m_1(m_1-m)+m_2(m_1+3m)]}{m_1(m+m_1)(m+m_2)}A_3+3(\frac{3}{m_1}-\frac{1}{m})B_{43}\right]
\end{aligned}$$

where

$$\begin{aligned}
A' &= p_f p_B(0)[\sqrt{3}p_{AC}(1,1)+2p_{AC}(0,0)] \\
B' &= p_B(0)[4\sqrt{3}v_{AC}(2,1,-1)+\sqrt{6}v_{AC}(1,1,0)-\sqrt{6}v_{AC}(1,0,-1)-2\sqrt{2}v_{AC}(0,1,1)+2\sqrt{2}v_{AC}(0,0,0)]
\end{aligned}$$

A.5 $F \to S + S$

- ${}^3F_4 \to {}^1S_0 + {}^1S_0$

$$
\begin{aligned}
M_s^{40} &= \frac{\sqrt{2\pi}b}{\sqrt{21}M_g^4}\left[-(\frac{1}{m+m_1}+\frac{1}{m+m_2})A_3+\frac{1}{2m}B_{44}\right] \\
M_v^{40} &= \frac{\sqrt{2\pi}\alpha_s}{3\sqrt{21}M_g^2}\left[\frac{2m(m_1-3m_2)-2m_1(m_1+m_2)}{m_1(m+m_1)(m+m_2)}A_3-3(\frac{1}{m_1}-\frac{1}{3m})B_{44}\right]
\end{aligned}
$$

References

1 Le Yaouanc A, Oliver L, Pene O, Raynal J C. Phys. Rev., 1973, **D8**: 2223–2234

2 Micu L. Nucl. Phys., 1969, **B10**: 521–526

3 Blundell H G, Godfrey S. Phys. Rev., 1996, **D53**: 3700–3711, `http://arxiv.org/abs/hep-ph/9508264` `arXiv:hep-ph/9508264`

4 Barnes T, Close F E, Page P R, Swanson E S. Phys. Rev., 1997, **D55**: 4157–4188, `http://arxiv.org/abs/hep-ph/9609339` `arXiv:hep-ph/9609339`

5 Blundell H G, *Meson properties in the quark model: A look at some outstanding problems*, Ph.D. thesis, Carleton University, 1996, `http://arxiv.org/abs/hep-ph/9608473` `arXiv:hep-ph/9608473`

6 Capstick S, Isgur N. Phys. Rev. D, 1986, **34**: 2809–2835

7 Capstick S, Roberts W. Phys. Rev. D, 1994, **49**: 4570–4586

8 Kokoski R, Isgur N. Phys. Rev., 1987, **D35**: 907

9 Eichten E, Gottfried K, Kinoshita T, Lane K D, Yan T M. Phys. Rev., 1978, **D17**: 3090

10 Ackleh E S, Barnes T, Swanson E S. Phys. Rev., 1996, **D54**: 6811–6829, `http://arxiv.org/abs/hep-ph/9604355` `arXiv:hep-ph/9604355`

11 Simonov Y A. `http://arxiv.org/abs/1103.4028` `arXiv:1103.4028 [hep-ph]`

12 Leinweber D B, Skullerud J I, Williams A G, Parrinello C (UKQCD). Phys. Rev., 1999, **D60**: 094507, `http://arxiv.org/abs/hep-lat/9811027` `arXiv:hep-lat/9811027`

13 Silva P J, Oliveira O. Nucl. Phys., 2004, **B690**: 177–198, `http://arxiv.org/abs/hep-lat/0403026` `arXiv:hep-lat/0403026`

14 Forshaw J R, Papavassiliou J, Parrinello C. Phys. Rev. D, 1999, **59**: 074008, `http://arxiv.org/abs/hep-ph/9808392` `arXiv:hep-ph/9808392`

15 Field J H. Phys. Rev. D, 2002, **66**: 013013, `http://arxiv.org/abs/hep-ph/0101158` `arXiv:hep-ph/0101158`

16 Godfrey S, Isgur N. Phys. Rev., 1985, **D32**: 189–231

17 Amsler C et al (Particle Data Group). Phys. Lett., 2008, **B667**: 1–1340